R-peaks detection based on stationary wavelet transform

Mostefa Merah, Abdelmalik Taleb-Ahmed, Hadj Larbi Beklaouz

Computer methods and programs in biomedicine 121 (2015) 149–160

R-peaks detection based on stationary wavelet transform

M. Merah[a,b,*], *T.A. Abdelmalik*[a,1], *B.H. Larbi*[c,2]

[a] *LAMIH, UMR CNRS 8201 UVHC Laboratory of industrial and Human Automation, Mechanics anc Computer Sciences, Université de Valenciennes et du Hainaut Cambrésis, Bat Malvache, 1er étage, bureau 204, Le mont Houy, 59313 Valenciennes Cedex 9, France*

[b] *Laboratoire Signaux et Images (LSI), Département Electronique, Faculté Génie Electrique Université USTO-MB, B.P 1505, El M'Naouar, Bir el Djir- Oran, Algeria*

[c] *Laboratoire Signaux et Systèmes (LSS), Université Abdelhamid Ibn Badis de Mostaganem, Route Belahcel, 27000 Mostaganem, Algeria*

Abstract :

Automatic detection of the QRS complexes/R-peaks in an electrocardiogram (ECG) signal is the most important step preceding any kind of ECG processing and analysis. The perfor-mance of these systems heavily relies on the accuracy of the QRS detector. The objective of present work is to drive a new robust method based on stationary wavelet transform (SWT) for R-peaks detection. The decimation of the coefficients at each level of the transformation algorithm is omitted, more samples in the coefficient sequences are available and hence a better outlier detection can be performed. Using the information of local maxima, minima and zero crossings of the fourth SWT coefficient detail, the proposed algorithm identifies the significant points for detection and delineation of the QRS complexes, as well as detection and identification of the QRS individual waves peaks of the pre-processed ECG signal.

Various experimental results show that the proposed algorithm exhibits reliable QRS detection as well as accurate ECG delineation, achieving excellent performance on different databases, on the MIT-BIH database (*Se* = 99.84%, *P* = 99.88%), on the QT Database (*Se* = 99.94%, *P* = 99.89%) and on MIT-BIH Noise Stress Test Database, (*Se* = 95.30%, *P* = 93.98%). Reliability and accuracy are close to the highest among the ones obtained in other studies. Experiments results being satisfactory, the SWT may represent a novel QRS detection tool, for a robust ECG signal analysis.

Keywords :

ECG

Wavelet transform

R-peaks detection

Stationary wavelet transform

(SWT)

1. Introduction

The electrocardiogram (ECG) is one of the most important tools in the diagnosis of heart diseases. In the ECG, QRS complex may be the most significant feature among all ECG features. This explains the fact that its automatic detection is the most important step preceding any kind of ECG processing and analysis (classification, some denoising algorithm, etc.). The performances of these systems heavily rely on the accu-

* *Corresponding author at*: LAMIH – Université de Valenciennes et du Hainaut-Cambrésis, le Mont Houy-Bât. Noël Malvache 59313 Valenciennes Cedex 9, France. Tel.: +33 0758808599/+213 0770760836.

E-mail addresses: merahmus@gmail.com (M. Merah), taleb@univ-valenciennes.fr (T.A. Abdelmalik), hadj70@yahoo.fr (B.H. Larbi).

[1] Tel.: +33 03 27 51 13 34/03 27 51 22 73; fax: +33 03 27 51 13 16; mobile: +33 0609936750.

[2] Tel.: +213 0771421312.

DOI : 10.1016/j.cmpb.2015.06.003

racy of the QRS complexes/R-peaks detector. However, due to the non-stationary of the ECG signal, the physiological conditions and the presence of many artifacts, finding a robust and general algorithm for ECG feature detection is a tough task. Therefore, many researchers have proposed a number of methods of the QRS complexes detection in the ECG in the past years, but none of them proves universally acceptable accuracy. Thus, efforts are constantly deployed for their enhancement. For instance, methods based on the wavelet transform (WT) [1–7].

The wavelet transformation is used for the signal decomposition, localized simultaneously in time and frequency by inducing a change of basis for the signal in question. Generally, in this approach, the R peak is located at a point being the local maxima of several consecutive dyadic wavelet scales [2]. Based on this principle, many other researches were published on the beat detection using a WT filtering step [1,3–7].

There are two kinds of wavelet transform, the Continuous Wavelet Transform (CWT) and the Discrete Wavelet Transform (DWT). The continuous wavelet transform contains redundant signal information. In addition, a consumption calculation of the CWT made in [8] showed that it is four times more power consuming than the digital wavelet computing. Although this fact would give priority to the use of the discrete wavelet transform in real-time automatic R peaks detection applications, DWT suffers from three major limitations; (1) shift sensitivity, (2) poor directionality, and (3) absence of phase information. In addition, when employing the wavelet transform for detection purposes, this approach has two important drawbacks, the lack of shift invariance and the loss of resolution at coarse scales. These problems can be avoided by using an *overcomplete wavelet transform*. The so-called *stationary wavelet transform* [9] achieves this by taking timeshifts equal to all integer values instead of two. Even if the use of the stationary wavelet transform (SWT) in the ECG signal denoising is subject of particular interest in recent research [10,11]. Its use in the ECG signal waves detection was rarely investigated. Hence, we propose in this paper, a robust method based on SWT for QRS complex detection. The obtained results are promising the algorithm is able to detect R peaks over different databases and outperforms the other algorithms evaluated on the same database, according to recent publications.

The paper is organized as follows: Section 2 provides details on the proposed algorithm, including an accurate description of the choice of the decision parameters such as the choice of the wavelet, the desired level of signal decomposition and the coefficients detail selection. This section also includes presentation of the SWT based QRS/R-peaks detection method. The proposed method is tested in Section 3, followed by the results discussion in Section 4. Finally, Section 5 concludes the paper.

2. Materials and methods

2.1. Dataset

To further evaluate the proposed algorithm and allow comparison with other studies, manually annotated ECG signals from various databases are used. The MIT-BIH Arrhythmia Database (MITDB) [12], the QTDB [14] and the MIT-BIH Noise Stress Test Database (NSTDB) [13]. In addition to the 48 records (109,494 beats) as in [1] from MITDB and the 12 records (25,590 beats) from NSTDB, 105 records (86,892 beats) from the QTDB are used. Each record of QTDB contains 2 ECG channels digitalized with a sampling frequency of 250 Hz.

2.2. Stationary wavelet transform

The SWT is also known by a variety of names in the literature including the dyadic wavelet transform (i.e. dyadic in scales), maximal overlap transform and the redundant wavelet transform. SWT is an offshoot of DWT whereby the scales are dyadic but the time steps are not subsampled at each level and hence are not dyadic. In terms of redundancy, the SWT is an intermediate representation of the high redundancy CWT and the nonredundant DWT. It maintains a dyadic sampling of the scales, and therefore maintains a non-redundancy frequency, but carries an almost continuous and uniform sampling time [15]. It has an interest in our study because; unlike the DWT, the redundant representation of SWT makes it shift-invariant and suitable for applications such as edge detection, denoising and data fusion. Since the decimation of its coefficients at each level of the transformation algorithm is omitted, more samples in the coefficient sequences are available, with equal length wavelet coefficients at each level, and hence a better detection can be performed. The DWT cannot provide this feature. Which is critical for a robust detection of the QRS complexes. The SWT has a similar tree structured implementation as DWT [16], without any decimation (sub-sampling) step as shown in Fig. 1. We can write a general transformation equation of SWT based on the coefficients $c_{j,k}$ calculated as follows:

$$c_{j,k} = \sum_{n \in z} x(n)\psi'_{j,k}(n), \tag{1}$$

where $\psi'_{j,k}(l)$ is the discrete wavelet defined by:

$$\psi'_{j,k}(l) = 2^{-(j/2)}\psi_{0,0}(2^{-j}(l-k)), \tag{2}$$

The wavelet coefficients are given by $ca_{j,k}$ *and* $cd_{j,k}$, which represent the approximate (scaling) coefficients and detail (wavelet) coefficients respectively, generated through the convolution chain of the original signal sequence $x(n)$ and level-adaptive size-varying highpass filter h^1 and lowpass filter g^1 respectively, as shown in Fig. 1.

Thus, the first scale and detail coefficients $ca_{1,k}$ and $cd_{1,k}$ of the SWT can be calculated from a convolution of the input

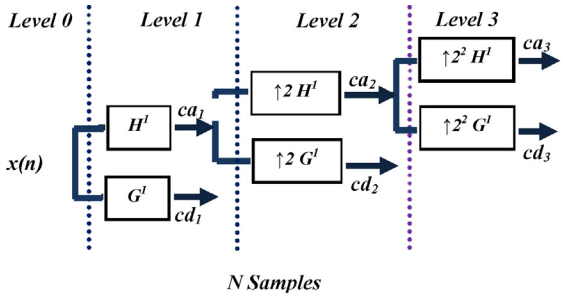

Fig. 1 – Three level decomposition with SWT.

signal $x(n)$ with highpass filter h^1 and lowpass filter g^1 respectively, as:

$$ca_{1,k}(n) = \sum h^1(n-\tau)x(\tau),$$
$$cd_{1,k}(n) = \sum g^1(n-\tau)x(\tau). \quad (3)$$

This can be generalized to the different coefficients scales by:

$$ca_{j,k}(n) = \left[\uparrow 2^{j-1}[h_1] * ca_{j-1,k}\right] = \sum h^j(n-\tau)ca_{j-1,k}(\tau),$$
$$cd_{j,k}(n) = \left[\uparrow 2^{j-1}[g_1] * ca_{j-1,k}\right](k) = \sum g^j(n-\tau)ad_{j-1,k}(\tau). \quad (4)$$

where $\uparrow 2^{j-1}[h_1] = h^j(n)$ is the over-sampling of the low-pass filter $h^{j-1}(n)$ coefficients and $\uparrow 2^{j-1}[g_1] = g^j(n)$ is the over-sampling of the high-pass filter $g^{j-1}(n)$ coefficients, which are given by:

$$\begin{cases} g^i(2n) = g^{i-1}(n) \\ g^i(2n+1) = 0 \\ h^i(2n) = h^{i-1}(n) \\ h^i(2n+1) = 0 \end{cases} \quad (5)$$

One can clearly see from the previous equation, that the highpass filter h^1 and lowpass filter g^1 are upsampled by a factor of two at each stage. Therefore, the decomposition coefficients (approximation and detail) have the same length Nc as the original signal $x(n)$, where $Nc = 2^j$, making the output signal more accurate than the one obtained with DWT.

2.3. *Decision parameters used in the proposed method*

2.3.1. *Wavelet choice*

Although a large variety of wavelets, are available, not all of them are suitable for peaks detection. There is no absolute rule for the choice of wavelets, but it is of utmost importance that the wavelet function corresponds closely to the processed signal [17].

In this work, the Daubechies2 wavelet is chosen because of its similar shape to the QRS complex and because of its energy spectrum is concentrated around the low frequencies [18]. The wavelet decomposition structure of MITDB record 100 up to 8 detail coefficients using Daubechies2 wavelet performed in [11] for denoising, is shown in Fig. 2.

A comparison between the original ECG signal and the reconstructed signal is also shown in Fig. 4.

2.3.2. *Level decomposition choice*

The level of the wavelet transform affects the number and location of peaks in a signal. Choosing the desired level of decomposition is connected to the frequency components necessary for the signal analysis over a given number of samples. Since SWT requires that the number of signal sample is a power of two, the following relationship must be satisfied:

$$2^N = n$$

where N = the total number of decomposition levels and n is the total number of the signal samples. Since most of the ECG signal energy is located within the first and fifth scale [11], the eighth scale is chosen in this study.

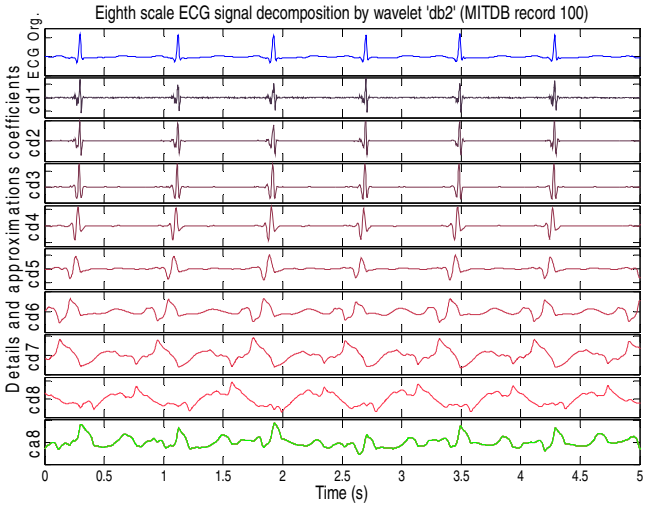

Fig. 2 – SWT at the eight scale of ECG signal using 'db2' wavelet for MITDB record 100.

2.3.3. *Detail coefficients choice*

While the mother wavelet can easily be chosen based on its characteristics and resemblance with a QRS wave, the ideal scale(s) at which the QRS are matched is harder to guess a priori. Thus, the several selections of detail coefficients for the detection of QRS complexes were proposed in the literature. In [19] Mahmoodabadi suggests the selection of details $d3$–$d5$ for R peaks detection. Saxena [18] in turn, uses the detail signal $d4$ for QRS peak detecting, while in the work of [20,1] five levels of wavelet, $d1$–$d5$, were used with a dyadic decomposition. Note that in all these works, DWT is used. In our case, the choice of detail coefficients is based on the following analysis.

2.3.3.1. Energy analysis. Most of the normal ECG signal energy is concentrated in a time interval of the QRS complex of about 80 ms, and in a frequency band ranging from 3 Hz to 40 Hz [19].

Fig. 3 shows the plot of the mean energy of the eight scales of the entire MITDB record database. One can see that it has a maximum at the level of the detail coefficient $cd4$, which

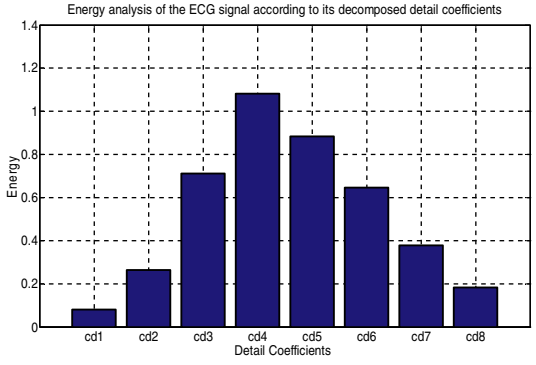

Fig. 3 – The mean energy of the SWT 8 scales of the entire MITDB record database.

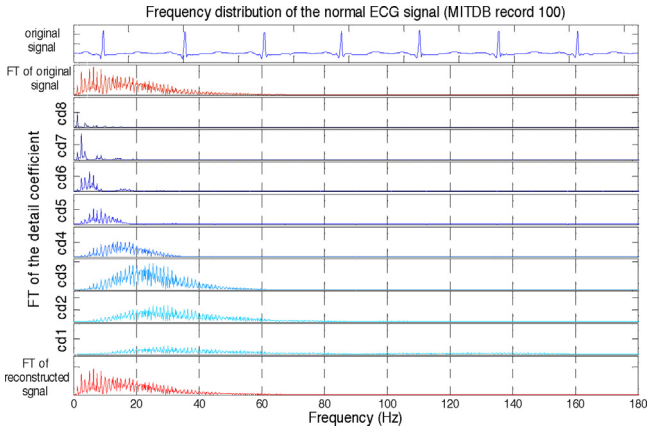

Fig. 4 – Frequency distribution of a normal ECG signal (MITDB record 100).

means that *cd*4 detail coefficient is a good candidate to be used in QRS complex detection.

2.3.3.2. *Frequency analysis*. Here, we look for the frequency components of the detail signals that is correlated with that of the QRS complex. For this, the Fourier transform of each detail signal is carried out. From Fig. 4, we observe that the bandwidth of the *cd*4 detail signal happens to be within 2.5–39.5 Hz, which is similar to that of the QRS complex.

According to this frequency distribution of the ECG signal, it can be noted that the high-frequency components of the ECG signal decreases as the lower order details removed from the original signal.

2.3.3.3. *Correlation analysis*. In addition to the above two analyses, the mean cross-correlation analysis between all detail signals and the original ECG signal of the entire MITDB record database was performed. This gives us a relationship in the time domain between the original QRS and the decomposed signals (signal details). The results are shown in Fig. 5.

From this figure, we can notice that the cross-correlation coefficient of detail *cd*4 has the highest value, which means that the detail coefficient signal *cd*4, is the best placed to

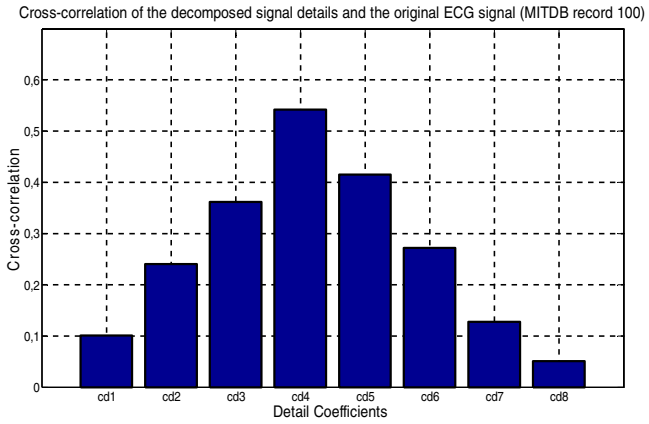

Fig. 5 – Mean cross-correlation analysis between detail of the decomposed signal and the original ECG signal of the entire MITDB record database.

approximated the QRS signal in the time domain. Finally, we can conclude that the detail coefficient *cd*4 is the best choice to be used for QRS detection.

2.4. *Methodology*

The objective of present work is to drive an algorithm for the detection of the QRS complex and the locating of the R peaks, using SWT. To achieve this objective the following processing are performed.

2.4.1. *Pre-processing*

ECG signals can be affected by various types of noise, such as motion artifacts, baseline drift, electromyogram (EMG), electrode motion artifact of even power-line interferences. These have to be suppressed during the analog data acquisition or afterwards in a digital signal preprocessing. Wavelet transform, due to its sparsity, locality, and multi-resolution nature, has emerged as a simply yet effective de-noising tool [1,3–5,7]. However, the disadvantage of filtering with WT with down sampling is that the result is dependent on the choice of the beginning of the filtering and the need for interpolation in reverse transform, which is always a source of errors. Thus, in this work the SWT, which preserves the length of the decomposed signal in all detail and approximation coefficient signals, is used. Based on [10,21], our ECG signals denoising algorithm, involves four main steps:

1. Removing the baseline wandering using DWT [7], by decomposition down to level 9, and using the wavelet filter Symlet 4.
2. Calculating the SWT for the noisy signal with a Symlet4 wavelet as basis function and decomposition up to 6 levels.
3. Zeroing or modifying certain coefficients by hard shrinkage function with Empirical Bayes posterior median thresholding.
4. Reconstructing the signal from the modified coefficients, with the aid of the Inverse Stationary Wavelet Transform (ISWT) to produce a denoised signal.

Performance of this algorithm is tested on NSTDB and evaluated based on Signal to Noise Ratio (SNR) and Mean Square Error (MSE) [22]:

$$\mathrm{SNR} = 10\log\frac{\sum_{N}^{i=1} x(i)^2}{\sum_{N}^{i=1}(x(i)-\bar{x}(i))^2} \tag{6}$$

$$\mathrm{MSE} = \frac{1}{N}\sum_{i=1}^{N}(x(i)-\bar{x}(i))^2 \tag{7}$$

where N is the length of the ECG signal, $x(i)$ is the simulated signal before noise is added and $\bar{x}(i)$ is the filtered signal with added noise. Fig. 6 shows the signal on record number 118e24 added with Gaussian noise, along with the denoised ECG signal. SNR value of noisy signals 118e24, was found to be 25.21 dB. Upon denoising with our approach, SNR value get enhanced to 34.4 dB and MSE value to 0.00073.

From above results, we can see that our de-noising algorithm provides a good noise suppression not only by mean of

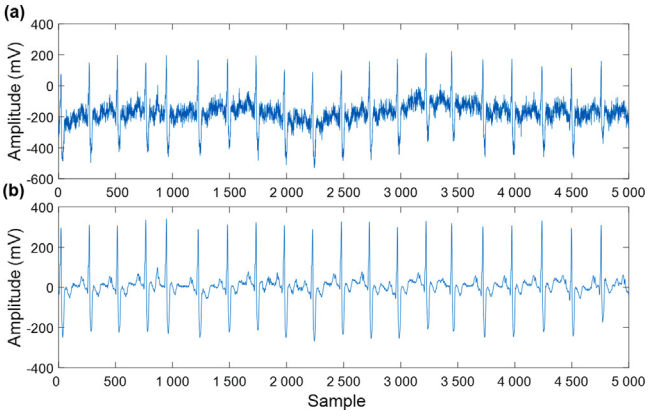

Fig. 6 – (a) Noisy ECG signal on record number 118e24 added with Gaussian noise, (b) denoised ECG signal using our approach.

visual inspection, but also by mean of SNR and MSE. Higher value of SNR and lower value of MSE shows that, the reconstructed ECG signal contains minimum distortion and depicts better noise suppression respectively.

2.4.2. *QRS complex detection and delineation*

Our algorithm, although based on the multiscale approach proposed by Li in [2] is quite different. One of the novelties with respect to [2] is that in our algorithm, a single scale (*cd*4) is taken into account. This scale was found to be the optimal common scale for the QRS complex detection. Using the information of local maxima, minima and zero crossings of the SWT at this scale, the algorithm identifies the significant points for detection and delineation of the QRS complexes, as well as detection and identification of the QRS individual waves (Q, R, S). From this representation, a decision rule is applied, defined as a search for a maxima modulus lines exceeding an adaptively threshold t_{QRS}. This threshold is proportional to RMS (root mean square) value of SWT squared detail coefficients *cd*4. Thus for the QRS complex detection, of each 2^{11} samples set we take:

$$t_{QRS} = 0.25RMS(cd4^2) \tag{8}$$

This amplitude threshold is used to define an evaluation window f_{QRS}. This window allows us to determine whether a pair of maxima modulus of opposite sign represent a QRS (see Fig. 7).

The size of the evaluation window f_{QRS}, is chosen equal to 40 ms in order to detect the most abrupt transitions in the ECG, i.e. the passage characteristic of the R-wave to S-wave in the QRS. In addition, in our context, a new detection of the signal is allowed only 200 ms after the previously detected QRS complex. This value corresponds to the duration of the refractory phase of the potential action. Another step in our approach is to eliminate the redundant or isolated maxima and minima by defining the new thresholds named γ_{QRS_n}, γ_{QRS_P}:

(a) The γ_{QRS_n} threshold is used to find negative significant slopes. It is proportional to the RMS value of SWT squared detail coefficients *cd*4 within the search window f_{QRS}:

$$\gamma_{QRS_n} = 0.4RMS(cd4(n)^2), \quad n \in f_{QRS} \tag{9}$$

(b) The γ_{QRS_P} threshold is used to find significant slopes of the S wave. It is proportional to RMS value of SWT squared detail coefficients *cd*4 within the search window f_{QRS}:

$$\gamma_{QRS_P} = 0.9RMS(cd4(n)^2), \quad n \in f_{QRS} \tag{10}$$

Thus, after rejecting all isolated or redundant (not significant) maxima modulus, the zero crossing of the SWT at the

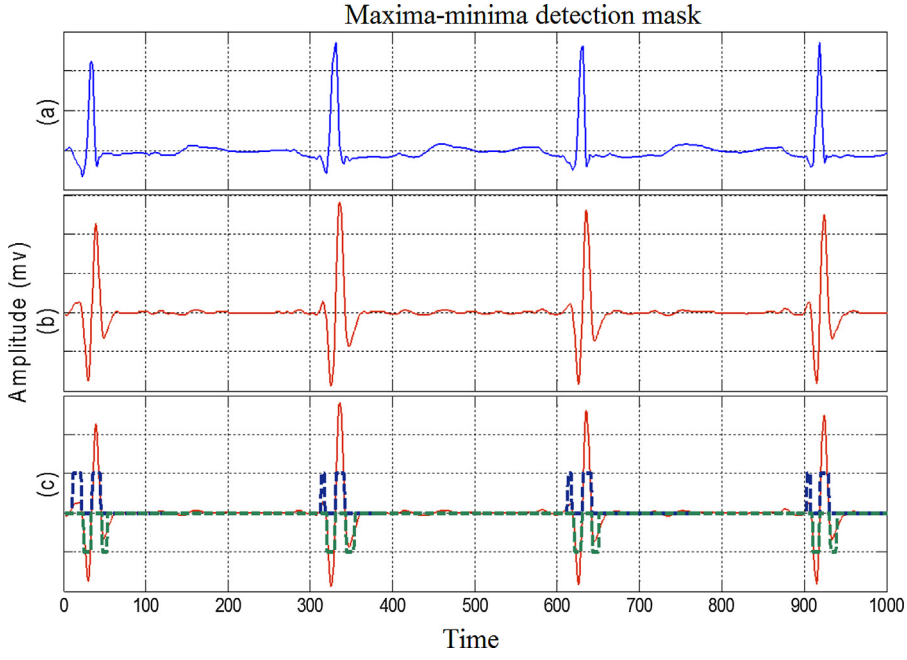

Fig. 7 – The maxima–minima detection mask.

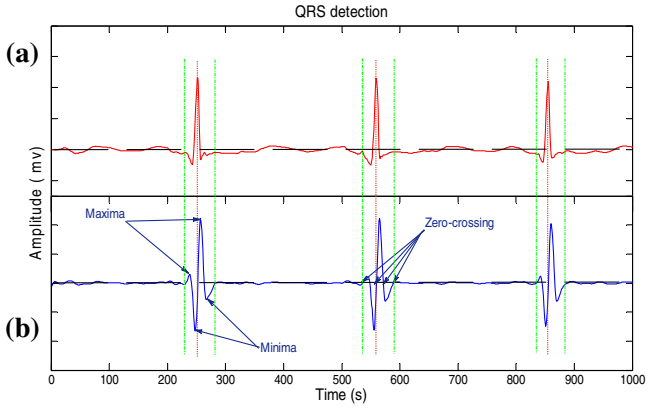

Fig. 8 – Maxima, minima and zero crossing in the detail signal *cd*4, for the QRS complex detection and delineation. (a)The ECG signal, (b) the detail coefficients *cd*4.

fourth scale between a positive maximum-negative minimum pair is marked as a QRS (Fig. 10). The QRS onset (end) is also defined by the zero crossing before (after) the first (last) significant slope of the QRS (Fig. 8).

In Fig. 9, some excerpts of the MITDB ECG records representing different kinds of QRS morphologies, have been chosen to illustrate the robustness of the proposed detector.

2.4.3. *QRS individual waves peaks detection and identification*

The algorithm departs from the position given by the QRS complex detector. The R-peak position of the original preprocessed signal is detected in the adjacent zero crossing located between the previously detected pair of maximum modulus with opposite signs at scale *cd*4 (see Fig. 10). This principle may also be used to detect the Q and S peaks. Since the detection of Q and S peaks is directly associated to the R-peak detection, the thresholds γ_{QRS_n}, γ_{QRS_P} being proportional to the maximum slope of the R wave, they are used to identify other significant slopes of the Q and S peaks.

In a normal QRS the locals minima of the Q and S peaks are located around the R-wave in the range of 0.12 millisecond (43 samples for a sampling rate of 360 Hz). This cannot be generalized to the pathological QRS. In this case the QRS complex is wide and has a length greater than 0.12 milliseconds; hence we increase of the interval search to 0.16 milliseconds. A last step of the R-peaks detection makes sure that Q and S spikes have not been wrongly labeled as a R. If two or more R spikes were detected in a window smaller than 250 ms (two heartbeats cannot physiologically happen in less than 250 ms [20]), the algorithm keeps only the peak which has the highest value on the original ECG.

3. Results

To evaluate the performance of the R peak detection algorithm we use rates including false negative (*FN*), which means failing to detect a true beat (QRS complexes have not been detected as QRS complexes), and false positive (*FP*), which represents a false beat detection (non-QRS complexes detected as QRS

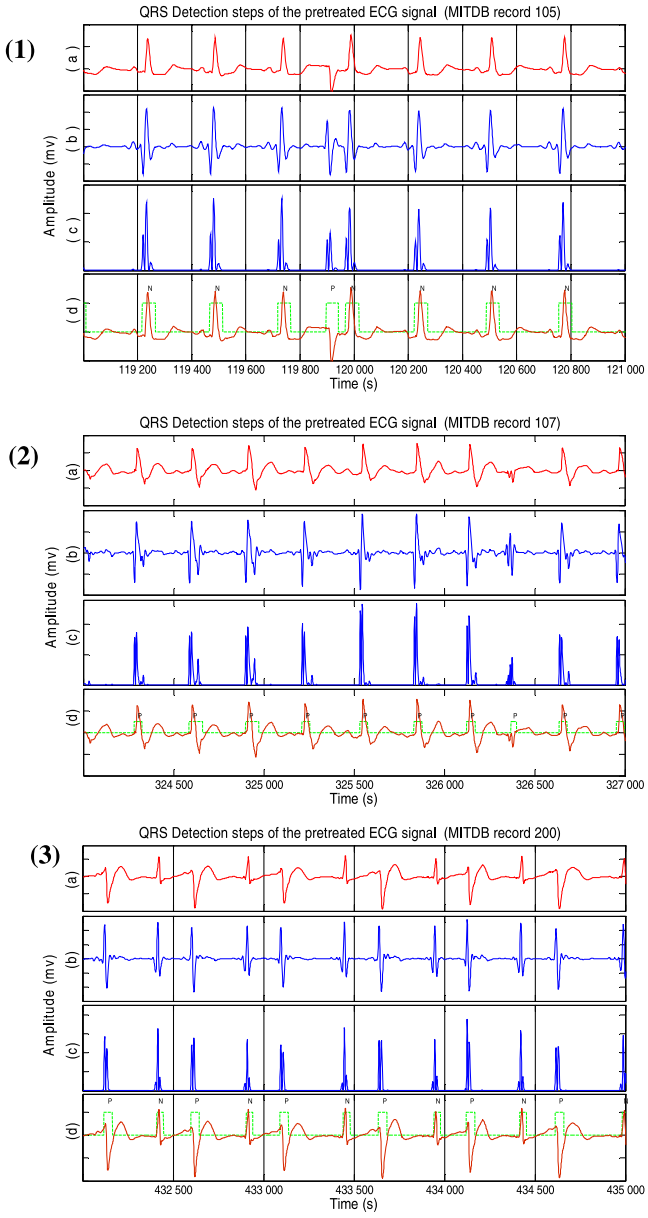

Fig. 9 – Examples of the detection step results, using different kinds of QRS morphologies. (1) MITDB record 105, (2) MITDB record 107, and (3) MITDB record 200. (a) The ECG signal, (b) the detail coefficients *cd*4, (c) the squared of the detail coefficients *cd*4 and (d) the detected QRS complexes (detecting window) and the MITBIH QRS annotation (P and N denote pathological and normal QRS respectively), are shown in each panel.

complexes). By using *FN* and *FP* the sensitivity (*SE*), positive prediction (+P) and detection error (*DER*) can be calculated using the following equations respectively, as suggested in [1]:

- The sensitivity measured by:

$$SE = \frac{TP}{TP + FN} \tag{11}$$

- the positive predictivity (+P) defined as:

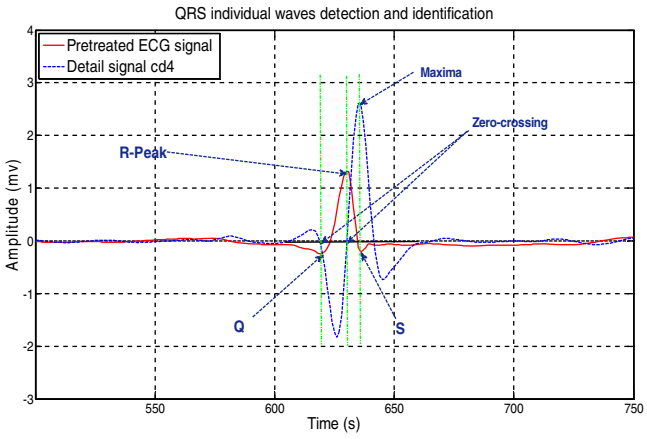

Fig. 10 – Illustration of the R, Q and S waves' detection.

$$+P = \frac{TP}{TP + FP} \tag{12}$$

- Detection error (DER) defined as:

$$DER = \frac{FP + FN}{TB}, \tag{13}$$

where *TP* is the number of true positives detections (QRS complexes detected as QRS complexes). The sensitivity (*SE*) reports the percentage of true beats that were correctly detected by the algorithm. The positive prediction (+*P*) reports the percentage of beat detections that were true beats.

These measures were determined by the decision-making rule that a beat is true when it is detected within a search window in our case 100 ms as in [23], from the annotated time for each record, otherwise false (in compliance with ANSI/AAMI-EC57:1998 standard).

Figs. 11–14 show an example of the Q, R and S peaks detection. The annotated and the detected waves are reported. Thus, a false positive occurs when the delineation process locates a characteristic point, which was not annotated. A false negative is considered when the delineation process fails to locate the annotated fiducial point within the above-mentioned tolerance.

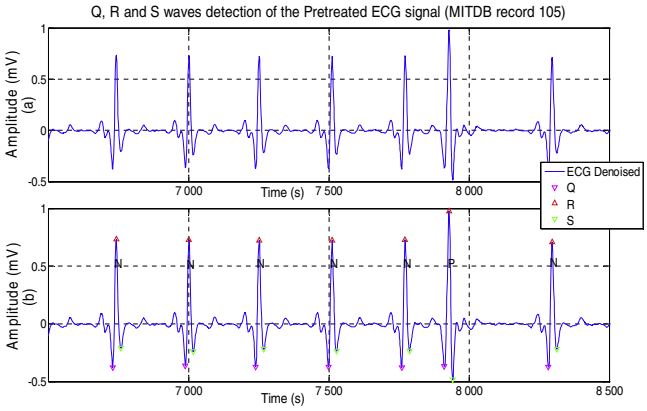

Fig. 11 – R Q, S wave detection results (MITDB record 105).

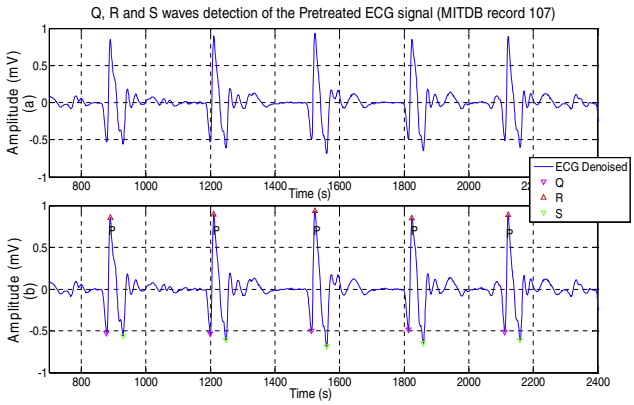

Fig. 12 – R Q, S wave detection results (MITDB record 107).

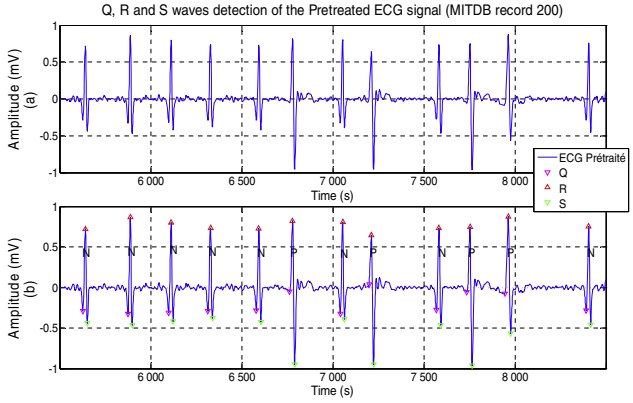

Fig. 13 – R Q, S wave detection results (MITDB record 200).

The R-peak detection rates for the first-channel (each) of 48 ECG recordings of the MITDB by our algorithm are summarized in Table 1.

The proposed method produces 178 *FN* beats and 126 *FP* beats for a total detection failure of 304 beats, and succeeded in detecting correctly 99.72% of the ECG beats. However, the individual detection accuracies of the ECG records vary from 98.64% to 100% depending on the characteristics of normal and pathological ECG signals, and different noises. In detail,

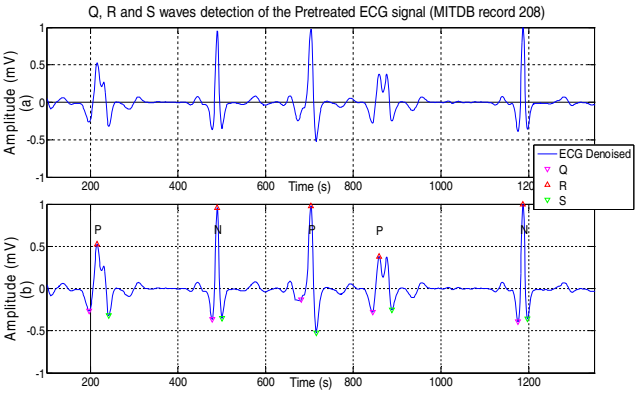

Fig. 14 – R Q, S wave detection results (MITDB record 208).

Table 1 – Performance of R detection algorithm on MITDB records.

Rec.	TB	TP	FP	FN	*Se* %	+P %	DER %
100	2273	2273	0	0	100	100	0.00
101	1865	1865	1	0	100	99.95	0.05
102	2187	2184	0	3	99.86	100	0.14
103	2084	2084	0	0	100	100	0.00
104	2229	2220	12	9	99.60	99.46	0.94
105	2572	2555	11	17	99.34	99.61	1.05
106	2027	2023	6	4	99.80	99.70	0.49
107	2137	2137	0	0	100	100	0.00
108	1763	1749	10	14	99.32	99.49	1.36
109	2532	2532	0	0	100	100	0.00
111	2124	2120	1	4	99.81	99.95	0.24
112	2539	2534	3	5	99.80	99.88	0.32
113	1795	1794	4	1	99.94	99.78	0.28
114	1879	1876	5	3	99.84	99.73	0.43
115	1953	1953	0	0	100	100	0.00
116	2412	2408	1	4	99.83	99.96	0.21
117	1535	1533	3	2	99.87	99.80	0.33
118	2278	2277	2	1	99.96	99.91	0.13
119	1987	1987	3	0	100	99.85	0.15
121	1863	1859	5	4	99.79	99.73	0.48
122	2476	2476	0	0	100	100	0.00
123	1518	1518	0	0	100	100	0.00
124	1619	1619	0	0	100	100	0.00
200	2601	2598	0	3	99.88	100	0.12
201	1963	1952	6	11	99.44	99.69	0.87
202	2136	2134	0	2	99.91	100.00	0.09
203	2980	2964	10	16	99.46	99.66	0.87
205	2656	2652	2	4	99.85	99.92	0.23
207	1860	1853	5	7	99.62	99.73	0.65
208	2955	2946	3	9	99.70	99.90	0.41
209	3005	3005	0	0	100	100	0.00
210	2650	2645	3	5	99.81	99.89	0.30
212	2748	2748	0	0	100	100	0.00
213	3251	3251	0	0	100	100	0.00
214	2262	2253	8	9	99.65	99.78	0.75
215	3363	3353	6	10	99.73	99.82	0.48
217	2208	2206	3	2	99.91	99.86	0.23
219	2154	2154	0	0	100	100	0.00
220	2048	2048	0	0	100	100	0.00
221	2427	2420	1	7	99.71	99.96	0.33
222	2483	2475	5	8	99.68	99.80	0.52
223	2605	2602	0	3	99.88	100.00	0.12
228	2053	2044	7	9	99.56	99.66	0.78
230	2256	2256	0	0	100	100	0.00
231	1571	1571	0	0	100	100	0.00
232	1780	1780	0	0	100	100	0.00
233	3079	3078	0	1	99.97	100	0.03
234	2753	2752	0	1	99.96	100	0.04
Total	109,494	109,316	126	178	99.84	99.88	0.28

we were able to achieve very high results such as the sensitivity of 99.84% and the positive predictive rate of 99.88%. Generally, detection problems may occur for the MITDB, ECG records 104, 105, 108, 200, 203, 210, and 228 containing, high-grade noise and artifact. Records 108, 111, 112, 116, 201, 203, 205, 208, 210, 217, 219, 222, and 228 including, severe baseline drifts and abrupt changes. Records 201, 202, 203, 219 and 222 exhibit various irregular rhythmic patterns. Records 201, 219 and 232 include long pauses up to 6 s in duration. Records 108 and 222 contain tall sharp P waves. Record 113 has tall sharp T waves. For these recordings, most algorithms have a quite high number of false positive detections. However, the proposed algorithm achieves a significant improvement in the detection of R-peak under time-varying QRS complex morphology and different kinds of noise and artifacts.

Thus, for the noisy records 104, 105, and 108. The proposed method has a total detection failure of 73 beats (33 *FP* beats and 40 *FN* beats). The Rec 201 has a detection failure rate of 0.87% (17 beats), and the Rec 203 has a detection failure rate of 0.87% (26 beats).

Next, a quantitative study of the noise tolerance test is performed. The performance of the proposed method with the presence of the noise was evaluated for the QRS-complex detection with the NSTDB [13], on records 118exx (2278 annotated beats) and records 119exx (1987 annotated beats) respectively (xx, being the SNR value). The performance of our

Table 2 – Noise-stress test using results of the proposed method on the NSTDB.

Rec.	TP	FP	FN	*Se* %	+P %	DER %
118e24	2277	2	1	99.96	99.91	0.13
118e18	2277	2	1	99.96	99.91	0.13
118e12	2268	27	10	99.56	98.82	1.62
118e06	2176	121	102	95.52	94.73	9.79
118e00	2105	227	173	92.41	90.27	17.56
118e_6	1997	345	281	87.66	85.27	27.48
119e24	1987	3	0	100.00	99.85	0.15
119e18	1987	3	0	100.00	99.85	0.15
119e12	1958	69	29	98.54	96.60	4.93
119e06	1906	117	81	95.92	94.22	9.96
119e00	1751	263	236	88.12	86.94	25.11
119e_6	1699	384	288	85.51	81.57	33.82
Total	24,388	1563	1202	95.30	93.98	10.81

detector is quit good for SNR as low as 6 dB with high sensitivity values (above 95%) as well as high positive prediction (about 95%). The results are depicted Table 2.

In compliance with [24] and to allow the use of the proposed algorithm on QTDB with the same sampling frequency, each record was re-sampled to 360 Hz using the "xform" program available from [13]. Table 3 shows the performance of the QRS detection algorithm on MITDB and QTDB. Moreover, it summarizes the performances across these databases and compares them to other reported results.

Referring to Table 3, it can be noticed that even if the performance of current R-peaks detection algorithms is not completely assessed in terms of parameter choice, and numerical efficiency, the performance of our algorithm, is located in a good enough position compared to the other methods, which used MITDB, NSTDB and QTDB ECG databases respectively.

Moreover, many of the QRS algorithms were not tested against a standard database or any database at all. Many researchers have excluded records from the MITDB [12] for the sake of reducing noise in the processed ECG signals; consequently, their algorithms appeared to achieve improved performance. This issue makes difficult to compare and evaluate the performance results of the proposed algorithm, with previously published algorithms. For example, it is worth noting that Li et al. [2] scored higher performance, a sensitivity of 99.89% and a specificity of 99.94%, than the proposed algorithm. This is because Li et al. excluded files 214 and 215 from the MITDB; the same can be formulated for the four methods that precede ours it can be noticed that their TB number is less than ours (see Table 3), and therefore their algorithm is not superior in terms of performance.

Here is an example based on the proposed detector: If records 105, 104 and 108 are excluded from this study, the proposed detector scores SE of 99.88% and VPP of 99.91%, which does not reflect the real performance of the algorithm. Thus, as discussed above, the number of records affects the overall accuracy of all detection algorithms.

In addition, the QTDB where the detector scored an SE of 99.94% and a +P of 99.89%, over 86,892 beats. The QRS detection accuracy is an important factor to be considered. Because the QRS contains most of information about cardiac and it is the basis of the complete delineation of ECG waveform. Thus, the performance of the detection and delineation of the QRS-complexes of the described methods was evaluated with the QTDB [14], according the metrics proposed in [1,4]. The mean μ and standard deviation σ (STD) of the differences between automatic detection and cardiologists annotations are computed in order to quantify the performance of the QRS detection algorithm (QRS onset and offset detection), in each ECG record. Moreover, as QTDB is widely used in the literature, the results using this database enable direct comparisons with state-of-the-art ECG delineation algorithms as shown in Table 4. The final row lists the tolerance limits for automatic feature extraction algorithms as were defined by the CSE Working party in [36].

4. Discussion

In this paper, the ECG records from three different databases are used to evaluate the proposed method. The MITDB is used to evaluate proposed methods for the R peaks detection. In particular, the sensitivity was used for evaluating the ability of the algorithm to detect true beats, the positive predictivity was used for evaluating the ability of the algorithm to discriminate between true and false beats, and the detection error rate was used for evaluating the accuracy of the algorithm. Unlike previous DWT based methods [1,2,4], the present only uses one scale (2^4), for QRS detection. Since the decimation of the coefficients at each level of the transformation algorithm is omitted, more samples in the coefficient sequences are available and hence a better outlier detection can be performed. The R-peaks detection showed an excellent performance on the MITDB, achieving a sensitivity of 99.84% and a positive predictive value of 99.88% on 109,494 annotated beats, as shown in Table 1.

In addition, the NSTDB is used to evaluate the noise sensitivity of the proposed R peaks detection method, and as expected, the results on the noise-stress test presented in Table 2, shows its immunity to the noise. This is mainly due to the effectiveness of the denoising algorithm used in this work [10], since it is known that a good pre-processing technique can basically help to improve the QRS peak detection [39].

As summarized in Table 2, our method indicate a good success rate for an SNR of more than or equal to 12 dB, where both the *Se* and the +*P* values are above 99%. The presented method still demonstrates an acceptable sensitivity and positive predictivity for an SNR of less than 12 dB, where *Se* value dropped below 96% and the +*P* value dropped below 95%.

Table 3 – Performance evaluation of QRS detection algorithms: application to MITDB, QTDB and NSTDB.

Methods	TB	TP	FP	FN	*Se* %	P+ %	DER %
MITDB							
Ghaffari et al., [5]	109,428	109,367	89	61	99.94	99.91	0.14
Liet al. [2]	104,182	104,070	65	112	99.89	99.94	0.17
Saxena et al. [18]	103,763	103,664	102	99	99.90	99.90	0.19
Li et al. [25]	109,497	109,430	138	67	99.94	99.87	0.19
Ning and Selesnick [26]	109,452	109,314	127	138	99.87	99.88	0.24
Zidelmal et al. [27]	108,494	108,323	97	171	99.84	99.91	0.25
SWT (this work)	109,494	109,316	126	178	99.84	99.88	0.28
Martinez et al. [1]	109,428	109,208	153	220	99.80	99.86	0.34
Ghaffari et al. [28]	109,428	109,215	160	213	99.80	99.85	0.34
Elgendi [29]	109,984	–	–	–	99.78	99.87	0.35
Cvikl et al. [30]	109,494	109,294	200	200	99.82	99.80	0.37
Hamilton and Tompkins [31]	109,267	108,927	248	340	99.69	99.77	0.54
QTDB							
Ghaffari et al. [5]	86,892	86,854	70	38	99.96	99.92	0.12
SWT (this work)	86,892	86,837	99	55	99.94	99.89	0.18
Ghaffari et al. [28]	86,892	86,819	94	73	99.92	99.89	0.19
Martinez et al. [1]	86,892	86,824	107	68	99.92	99.88	0.20
Moody et al. [32]	86,892	84,458	459	2434	97.2	99.46	3.33
NSTDB							
SWT (this work)	25,590	24,388	1563	1202	95.30	93.98	10.81
Benitez et al. [33]	–	–	–	–	93.48	90.60	–
Li and Tan [34] ROSA	–	–	–	–	90.67	87.19	–
Li and Tan [34] S.S.A	–	–	–	–	98.64	77.61	–
Plesnik et al. [35] der-area	27,455	24,913	4407	2542	90.74	84.97	25.31
Plesnik et al. [35] der-euc	25,117	21,703	3241	3414	86.41	87.01	26.50

der-euc: The method is based on the Euclidean distance calculation in the phase space.
der-area: The method is based on the area calculation in the phase space.
S.S.A (Single scan algorithm): differentiator, digital low-pass filter and an and decision rules.
ROSA 5Robust open-source algorithm: low-pass filter, nonlinearly scaled curve length transformation (LT), and decision rules.

As shown in Table 3, the algorithm was able to achieve very high results comparable to [33–35] indicating a sensitivity of 95.30% and positive predictive rate of 93.98% on 25,590 annotated beats. One can notice, that even the second method proposed by Li [34] indicate the best sensitivity value (98.64%), its shows also the worst positive predictivity value (77.61%). From these results, it can be concluded that our algorithm achieves the best results for noisy ECG signals, while reasonably preserving the clinical features of ECG signals at the same time.

Table 4 – Evaluation and comparison of delineation performance of the algorithms with published methods (QTDB).

Method	QRS_{ON} $(\mu \pm \sigma)$ (ms)	R peak $(\mu \pm \sigma)$ (ms)	QRS_{OFF} $(\mu \pm \sigma)$ (ms)
Ghaffari et al. [5]	-0.6 ± 4.9	0.7 ± 2.4	-0.1 ± 5.9
SWT	-1.1 ± 5.2	0.6 ± 2.2	0.2 ± 6
Ghaffari et al. [28]	-0.6 ± 8.0	1.1 ± 2.8	0.3 ± 8.8
Martinez et al. [1]	4.6 ± 7.7	–	0.8 ± 8.7
Laguna et al. [37]	-3.6 ± 8.6	–	-1.1 ± 8.3
Boichat et al. [4]	3.4 ± 7.0	–	3.5 ± 8.3
Mazomenos et al. [38]	3.7 ± 7.8	3.8 ± 9.8	12.1 ± 16.6
CSE [36] Tolerance (2σ)	6.5	–	11.6

Furthermore, in order to check the reliability of our algorithm, we tried to compare our work with other works on the QTDB. The QRS detection performance of four selected algorithms together with our algorithm are summarized in Table 3. With a sensitivity about 99.94%, positive predictive equal to 99.89% and detection error rate of (0.18%), the proposed algorithm among the compared algorithms shows the second best detection error rate behind the algorithm proposed by Ghaffari et al. [5] (0.12%). Here, we should mention that the underling result is very encouraging since each of the 105 records were re-sampled from 250 Hz to 360 Hz.

In the present work, the width of the search window adopted in the computation of *TP* was set to 100 ms [22]. The use of this window gave similar result to those with a wider windows (for instance, in [4] the width of the search window was set to 320 ms), since the SWT preserves the important time aspect of the non-stationary ECG signal.

Sensitivity and positive predictive value of the ECG R-peak detector were comparable to the values reported by others, as shown in Table 3. Previous DWT-based methods [1,2], compute the adaptive thresholds in QRS detection t_{QRS} based on the root mean square of d_n coefficients at the scales of interest. In [1] RMS is computed over $N = 2^{16}$ samples excerpts, for the first three scales (2^1, 2^2, 2^3). In [2] RMS is emulated over $N = 2^9$ samples excerpts for the first four scales. RMS is computationally demanding, as it requires squaring and summing N coefficients and calculating a square root. Although the square root was emulated in [2], a considerable amount of

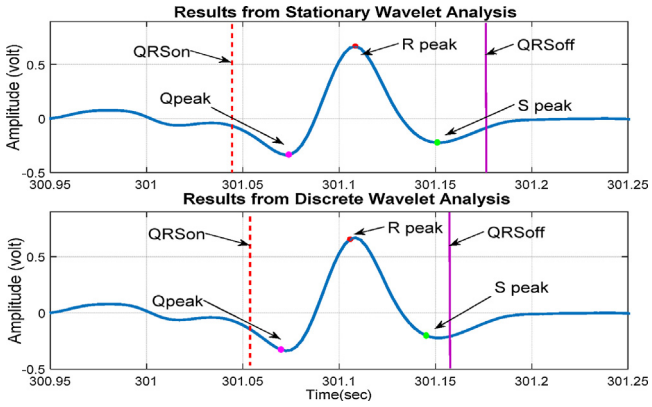

Fig. 15 – Discrete wavelet transforms vs stationary wavelet transforms for QRS fiducial points estimation.

computations is required for squaring large data excerpts. In the present method, which uses only one scale, all thresholds are calculated from few (local) coefficients, which dramatically reduce the computational effort. In particular, the computation of t_{QRS} by (6) only requires $N = 2^4$ data-points, compared to $N = 2^9$ in [2] and $N = 2^{16}$ in [1]. This observation also applies to γ_{QRS_n} and γ_{QRS_P}.

Table 4 lists accuracy results for QRS delineation attained from executing the proposed algorithm on 105 records from the QTDB. It shows that, in terms of standard deviation σ and mean error μ, which were around 4.5 ms (1.6 samples, at $F_s = 360$ samples/s), and lower than 2 ms (0.7 samples) respectively, the proposed algorithm, is around tolerances accepted by cardiologists [36], and slightly outperforms the other compared algorithms, when evaluated on the QT database, except the one proposed by [5].

Furthermore, in order to check the accuracy of the proposed algorithm for localization of the main deflection (either R peak or Q, S peak) and of the QRS boundaries. We design two algorithms: select the same wavelet basic, decomposition level, and thresholding method, but different transforms (DWT and SWT) respectively, and compare the QRS fiducial points estimation results, as shows in Fig. 15.

The result depicted in Fig. 15 was expected. Since the temporal resolution on the 2^4 scale of the DWT is diminished (by a factor of 16) compared to the original timescale, this coupled with fact that we operate on a single resolution scale, and the need for interpolation in reverse transform, may inherently lead to less accurate estimation of the QRS fiducial points. In addition, since the SWT preserve the length of the decomposed signal in all detail and approximation coefficient signals, it lead to more accurate localization of R, Q and S peaks, as the QRS boundaries.

5. Conclusions

In this paper, a discrete stationary wavelet transform for the automatic detection of R-Peaks in ECG is introduced. The algorithm exploits the translations invariance of the SWT, which preserves the important time aspect of the non-stationary ECG signal, and is effective because it takes into account the nonstationarity of the signal. In order to reduce the computational complexity, only the coefficients at scale 2^4 obtained by the SWT is applied to detect the R-Peaks. It has the advantage, to have a same sampling time of the signal with respect to the DWT.

The performance of the proposed method is promising. It has been tested on different databases, with the MITDB and the QTDB for the R-peaks detection and QRS-complex delineation and the NSTDB for the noise sensitivity. The presented method achieved excellent performance on the MITDB ($Se = 99.84\%$, $P = 99.88\%$). The validation results with QTDB are good enough to meet the demand for QRS-complex detection ($Se = 99.94\%$, $P = 99.89\%$). Evaluation results on the NSTDB indicate that the algorithm is effective ($Se = 95.30\%$, $P = 93.98\%$). This confirms that the SWT filtering is sufficient for effective QRS detection in signals contaminated with higher noise amplitudes. Thus, this reliable robustness against strong noise, artifacts and probable severe arrhythmia(s) of NSTDB can be mentioned as important merits and capabilities of the proposed algorithm.

This new algorithm also exhibited very good accuracy in QRS delineator on QTDB, where the mean error between automatic and manual annotations was lower than 1 samples for all the characteristic points, and the associated average standard deviations outperforms the other algorithms evaluated on the same database, according to recent publications.

REFERENCES

[1] J.P. Martínez, R. Almeida, S. Olmos, A.P. Rocha, P. Laguna, A wavelet-based ECG delineator: evaluation on standard databases, IEEE Trans. Biomed. Eng. 51 (4) (2004) 570–581.

[2] C. Li, C. Zheng, C. Tai, Detection of ECG characteristic points using wavelet transform, IEEE Trans. Biomed. 42 (1) (1995) 21–28.

[3] M. Ayat, M.B. Shamsollahi, B. Mozaffari, S. Kharabian, ECG denoising using modulus maxima of wavelet transform, in: Conf. Proc. IEEE Eng. Med. Biol. Soc., 2009, pp. 416–419.

[4] N. Boichat, N. Khaled, F. Rincon, D. Atienza, Wavelet-based ECG delineation on a wearable embedded sensor platform, in: Proc. 6th IEEE Int. Work. Body-Sen. Net., 2009, pp. 256–261.

[5] A. Ghaffari, M.R. Homaeinezhad, M. Khazraee, M. Daevaeiha, Segmentation of holter ECG waves via analysis of a discrete wavelet derived multiple skewness-kurtosis based metric, Ann. Biomed. Eng. 38 (4) (2010) 1497–1510.

[6] H.Q. Li, X.F. Wang, Detection of electrocardiogram characteristic points using lifting wavelet transform and Hilbert transform, Trans. Inst. Meas. Control 35 (5) (2013) 574–582.

[7] D. Zhang, Wavelet approach for ECG baseline wander correction and noise reduction, in: 27th Ann. Int. Conf. Eng. Med. Biol. Soc. IEEE-EMBS, 2005, pp. 1212–1215.

[8] V. Simard, B. Gosselin, M. Sawan, An analog wavelet processor for a fully implantable cortical signals recording system, in: Proc. of the Vien. 8th Int. Work. FES, 2004, pp. 164–167.

[9] G.P. Nason, B.W. Silverman, The stationary wavelet transform and some statistical applications Anestis. Antoniad. George. Oppenh. Edit. Lec. Note. Stat. Wav. Stat., 103, 1995, pp. 281–299.

[10] S. Li, J. Lin, The optimal de-noising algorithm for ECG using stationary wavelet transform, WRI World Congr. Comput. Sci. Inf. Eng. 6 (1) (2009) 469–473.

[11] B. Arvinti, M. Costache, D. Toader, M. Oltean, A. Isar:, ECG statistical denoising in the wavelet domain, in: 9th International Symposium on Electronics and Telecommunications, IEEE, 2010, pp. 307–310.
[12] R. Mark, G. Moody, MIT-BIH arrhythmia database. Available from: http://www.physionet.org/physiobank/database/mitdb/ (accessed 28.08.14).
[13] A.L. Goldberger, L.A.N. Amaral, L. Glass, J.M. Hausdorff, P.Ch. Ivanov, R.G. Mark, J.E. Mietus, G.B. Moody, C.K. Peng, H.E. Stanley, PhysioBank, PhysioToolkit, and PhysioNet: components of a new research resource for complex physiologic signals, Circulation 101 (23) (2000) e215–e220.
[14] P. Laguna, R.G. Mark, A. Goldberg, G.B. Moody, A database for evaluation of algorithms for measurement of QT and other waveform intervals in the ECG, Comput. Cardiol. (1997) 673–676.
[15] J.C. Pesquet, H. Krim, H. Carfatan, Time-invariant orthonormal wavelet representations, IEEE Trans. Sig. Process. 44 (1996) 1964–1970.
[16] S. Mallat, A Wavelet Tour of Signal Processing, Acad. Press, San Diego, CA, 1999.
[17] A. Grap, An introduction to wavelets, IEEE Comput. Sci. Eng. 2 (2) (1995).
[18] S.C. Saxena, V. Kumar, S.T. Hamde, Feature extraction from ECG signals using wavelet transforms for disease diagnostics, Int. J. Syst. Sci. 33 (13) (2002) 1073–1085.
[19] S.Z. Mahmoodabadi, A. Ahmadian, M.D. Abolhasani, M. Eslami, J.H. Bidgoli, ECG feature extraction based on multiresolution wavelet transform, in: Conf. Proc. IEEE Eng. Med. Biol. Soc., 2005, pp. 3902–3905.
[20] I.I. Christov, Real time electrocardiogram QRS detection using combined adaptive threshold, Biomed. Eng. Online 3 (28) (2004) 1–9.
[21] M. Merah, A. Ouamri, A. Nait-ali, M. Keche, Fault tolerant neural network for ECG signal classification systems, Adv. Electr. Comput. Eng. 11 (3) (2011) 17–24.
[22] R.D. Mali, M.S. Khadtare, U.L. Bombale, Removal of 50 Hz PLI using discrete wavelet transform for quality diagnosis of biomedical ECG signal, Int. J. Comput. Appl. 23 (7) (2011) 1–6.
[23] C. Meyer, J.F. Gavela, M. Harris, Combining algorithms in automatic detection of QRS complexes in ECG signals, IEEE Trans. Inf. Technol. Biomed. 10 (3) (2006) 468–475.
[24] American National Standard for Testing and Reporting, Performance Results of Cardiac Rhythm and ST Segment Measurement Algorithms, AAMI/ANSI Standard EC57:1998, 1998.
[25] H. Li, X. Wang, L. Chen, E. Li, Denoising and R-peak detection of electrocardiogram signal based on EMD and improved approximate envelope, Circuits Syst. Sig. Process. 4 (33) (2014) 1261–1276.
[26] X. Ning, I.W. Selesnick, ECG enhancement and QRS detection based on sparse derivatives, Biomed. Sig. Process. Control 8 (1) (2013) 713–723.
[27] Z. Zidelmal, A. Amirou, D. Ould Abdeslam, A. Moukadem, A. Dieterlen, QRS detection using S-Transform and Shannon energy, Comput. Methods Programs Biomed. 116 (1) (2014) 1–9.
[28] A. Ghaffari, M.R. Homaeinezhad, M. Atarod, M. Akraminia, Parallel processing of ECG and blood pressure waveforms for detection of acute hypotensive episodes: a simulation study using a risk scoring model, Comput. Methods Biomech. Biomed. Eng. 13 (2) (2010) 197–213.
[29] M. Elgendi, Fast QRS detection with an optimized knowledge-based method: evaluation on 11 standard ECG databases, PLOS ONE 8 (9) (2013) e73557.
[30] M. Cvikl, F. Jager, A. Zemva, Hardware implementation of a modified delay-coordinate mapping-based QRS complex detection algorithm, EURASIP J. Adv. Sig. Process. 1 (2007) 1–14.
[31] P.S. Hamilton, W. Tompkins, Quantitative investigation of QRS detection rules using the MIT/BIH arrhythmia database, IEEE Trans. Biomed. Eng. 33 (12) (1986) 1157–1165.
[32] G.B. Moody, R.G. Mark, Development and evaluation of a 2-lead ECG analysis program, Comput. Cardiol. (1982) 39–44.
[33] D.S. Benitez, P.A. Gaydecki, A. Zaidi, A.P. Fitzpatrick, A new QRS detection algorithm based on the Hilbert transform, Comput. Cardiol. (2000) 379–382.
[34] H. Li, J. Tan, Body sensor network based context aware QRS detection, in: Proc. 28th IEEE EMBS Ann. Int. Conf., New York, USA, 2006, pp. 3266–3269.
[35] E. Plesnik, O. Malgina, J.F. Tasic, S. Tomazi, M. Zajc, Detection and delineation of the electrocardiogram QRS-complexes from phase portraits constructed with the derivative rule, Exp. Clin. Cardiol. 20 (8) (2014) 2980–2989.
[36] C.S.E. Working Party, Recommendations for measurements standards in quantitative electrocardiography, Eur. Heart J. 6 (1) (1985) 815–825.
[37] P. Laguna, R. Jané, P. Caminal, Automatic detection of wave boundaries in multilead ECG signals: validation with the CSE database, Comput. Biomed. Res. 27 (1) (1994) 45–60.
[38] E.B. Mazomenos, D. Biswas, A. Acharyya, et al., A low-complexity ECG feature extraction algorithm for mobile healthcare applications, IEEE J. Biomed. Heal. Inf. 17 (1) (2013) 459–469.
[39] A. Binti, M. Binti, A.B. Ghani, Development of a concept demonstrator for QRS complex detection using combined algorithms, Biomed. Eng. Sci. IECBES (2012) 689–693.